



**Publication**

ALICE reference number

ALICE-PUB-2001-49 version 1.0

Institute reference number

Date of last change

2001-10-19

**The Gassiplex0.7-2 Integrated Front-End Analog  
Processor for the HMPID and the  
Dimuon Spectrometer of ALICE**

**Author:**

J.C. Santiard, K. Marent  
for the ALICE Collaboration

# THE GASSIPLEX0.7-2 INTEGRATED FRONT-END ANALOG PROCESSOR FOR THE HMPID AND THE DIMUON SPECTROMETER OF ALICE

J.C. Santiard, CERN, Geneva, Switzerland (Jean-Claude.Santiard@cern.ch)  
K. Marent, IMEC vzw, 3001 Leuven, Belgium (marentk@imec.be)

## ABSTRACT

The most recent member of the Gaspex family of ASICs has been designed in a 0.7  $\mu\text{m}$  n-well CMOS process to meet specifications for the ALICE applications: 500 fC linear dynamic range and a peaking time of 1.2  $\mu\text{s}$ . Its internal circuitry is optimized for the readout of gaseous detectors. A dedicated filter compensates the long hyperbolic signal tail produced by the slow drift of the ions and allows the shaper to achieve perfect return to the base line after 5  $\mu\text{s}$ . Measurement of fabricated chips showed a noise performance of 530  $e^-$  rms at 0 pF external input capacitance and 1.2  $\mu\text{s}$  peaking-time, with a noise slope of 11.2  $e^-$  rms/pF. The gain is 3.6 mV/fC over a linear dynamic range of 560 fC.

## 1. INTRODUCTION

Since the AMPLEX[1], the benefit of using multiplexed analog integrated circuits as front-end for the readout of gaseous detectors, has been widely proved. Its main feature was to use the peaking time of the shaped signal as a delay, allowing an external trigger to memorise the information by a Track-and-Hold circuit. Based on the same technique, the GASPLEX[2] was the first monolithic circuit for which the pulse shaping was adapted to the special signal of gaseous detectors. A simplified version of the GASPLEX, the GASSIPLEX1.5, manufactured with a volume production of 60 wafers, has a simpler logic I/O levels with the same functionality and internal shaping. The more recent version presented in this paper, the GASSIPLEX0.7-2, has been designed in a 0.7  $\mu\text{m}$  n-well CMOS technology with a peaking time of 1.2 $\mu\text{s}$  and an extended dynamic range of 500 fC. The analog circuitry follows the same principle as the GASPLEX: a Charge Sensitive Amplifier (CSA) with a long decay-time in order to collect the largest part of the detector signal.

After the CSA, a deconvolution filter compensates the logarithmic shape of the charge signal and provides the shaper with a quasi-step function with one pole given by the  $R_f.C_f$  time constant of the CSA.

The shaper provides a Semi-Gaussian signal with a 1.2 $\mu\text{s}$  peaking-time and a return to the baseline better than 1% after 5 $\mu\text{s}$ . A track-and-hold circuit stores the

analog information at the peaking time and finally the 16 channels are multiplexed to one output.

The Gassiplex0.7-2 also provides an individual channel calibration with a precision better than 1.5%.

## 2. CIRCUIT DESCRIPTION

The Gassiplex0.7-2 is a 16-channel low noise signal processor. It has been developed to fit the requirements of two ALICE detectors: the HMPID[3] which uses the Ring Imaging Cerenkov (RICH) technique and the dimuon spectrometer[4].

Both detectors utilise Multiwire Proportional Chambers with cathode pad or cathode strip readout.

In gaseous detectors, the ion cloud released by the avalanche around the anode wires induces current as long as it drifts in the electric field from the anode to the cathode. The charge close to the anode can be approximated by the expression  $q(t) = Q_0 A \ln(1+t/t_0)$  and the current by  $i(t) = I_0 B / (1+t/t_0)$ , where  $Q_0$  is the total ionic charge and  $A$ ,  $B$  and  $t_0$  are constants depending on the detector geometry and the electric field.

The following diagrams show the different blocks of the channel circuitry: CSA, deconvolver and shaper.

The CSA is made of two main parts: a folded cascode stage and an active feedback resistor. The input transistor is a p-channel with a W/L of 4000; coupled with the folded transistor it allows to work with a large range of detector capacitance, and exhibits good performances at relatively low power budget.

The feedback resistor has been implemented with a 50k $\Omega$  high ohmic silicon layer, followed by a current divider of 400; coupled with the feedback capacitance, it results in a decay-time constant of 20 $\mu\text{s}$ .

After the CSA, a deconvolution filter has been implemented to compensate the long tail resulting from the ions drift. The detector can be modelled as a linear system with an impulse response  $h(t) = U(t)/(t_0+t)$  stimulated by a Dirac pulse  $i_s(t) = Q_0 \delta(t)$ ,  $U(t)$  being a step function. To perform the deconvolution, the transfer function of the deconvolver  $G(s)$  should be the exact inverse of the transfer function of the detector  $H(s)$ , namely  $G(s) = H(s)^{-1}$ , where  $H(s)$  is the Laplace transform of  $h(t)$ .

The charge given by the detector is approximated by the sum of three weighted exponentials [5]. Each exponential is modelled by a pole (OTA1, OTA2)

placed in the feedback of a summing amplifier (SUM\_OTA) to implement the inverse transformation:  $G(s) = V_{out}/V_{in} = A/(1+\beta A)$ ; for A large  $G(s) \sim 1/\beta$  and  $\beta = K_1/(1+sT_1) + K_2/(1+sT_2) + K_3/(1+sT_3)$ . Notice that the third exponential is internal at SUM\_OTA. After deconvolution the filter output looks like a step function with one pole given by the  $R_f.C_f$  decay-time constant of the CSA. It allows the shaper to maintain a stable and precise return to the base line.

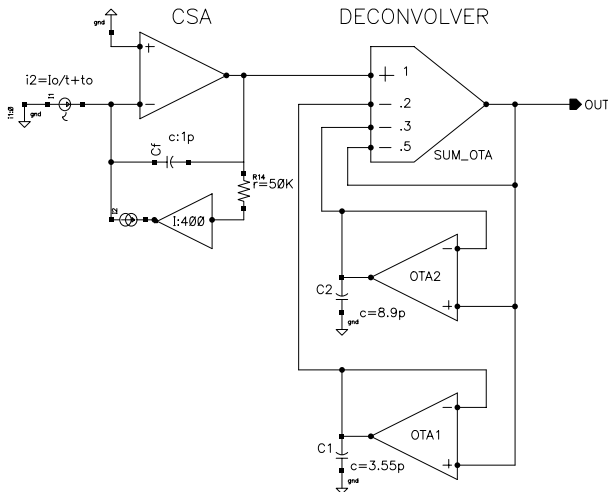


Fig 1: CSA and Filter blocks

The shaper circuit shown in fig. 2 has an original feature: from the output of the filter two different integrating paths are compared at the inputs of an amplifier (OTA4); it results in a Semi-Gaussian shape and thereby eliminates the usual differentiation capacitor.

Owing to the pole given by the time-constant of the CSA ( $R_f.C_f$ ), it is necessary to introduce a zero in the transfer function of the shaper. This is done on the output of OTA5 with an active resistor  $R_p/z$ . The cancellation occurs when the two time-constants are equal: thus,  $R_p/z = R_f.C_f/C_5$ ,  $C_5$  being 9 pF gives  $R_p/z = 2.22$  MΩ. This resistor is equivalent to the feedback resistor of the CSA and shares the same biasing.

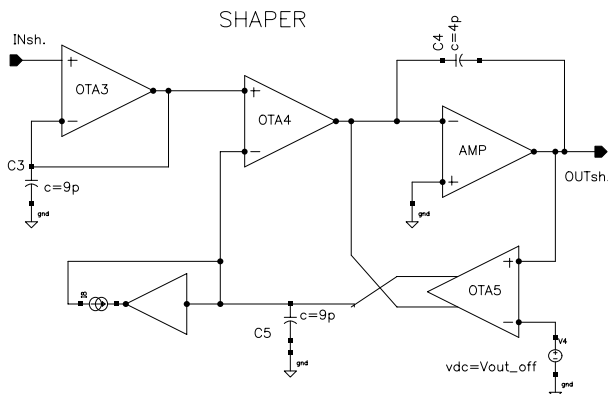


Fig 2: Shaper block

Fig. 3 shows the signals at different points of the circuit: at the outputs of the CSA, Filter and Shaper.

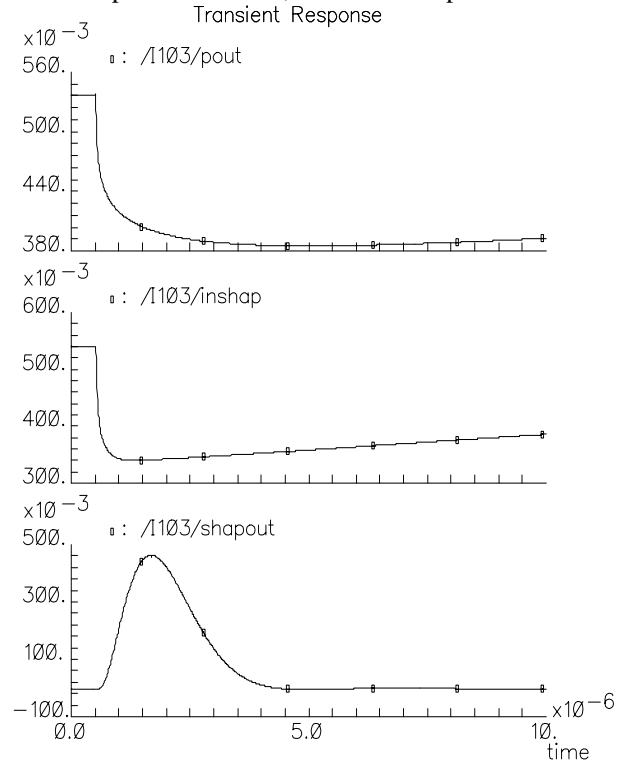


Fig 3: CSA, Filter and Shaper output signal shape

In addition, the Gassiplex07-2 provides individual channel calibration. Each channel has a 1pF-injection capacitor coupled to an analog switch activated by a shift register. The accuracy of the calibration circuit reflects the fact that capacitances are the most accurate elements in a CMOS process.

This calibration input multiplexer as well as the output multiplexer provide a Clock-out output which can be used to daisy-chain several chips (four in the Alice case), the analog output being common. The Clock-out of a chip is equal to the Clock-in minus the 16 clocks that perform the readout of the chip.

Finally another important feature is the possibility to switch-off the deconvolution filter in case of using a Silicon detector. Notice that if the detector leakage current is bigger than 1nA, a coupling capacitor is needed between the inputs of the Gassiplex07-2 and the detector.

### 3. MEASUREMENTS RESULTS

Measurements have been done on several chips coming from two wafers; the results were slightly different, but not distinguished in the measurements presented here.

#### 3.1 Noise versus input capacitance

The noise measurements (fig. 4) have been performed at a power consumption of 8mW/channel

with 350  $\mu\text{A}$  drawn by the input transistor and a peaking time of 1.2  $\mu\text{s}$ . It resulted in a noise slope of 11.2  $e^-$  rms and a residual noise of 470  $e^-$  rms.

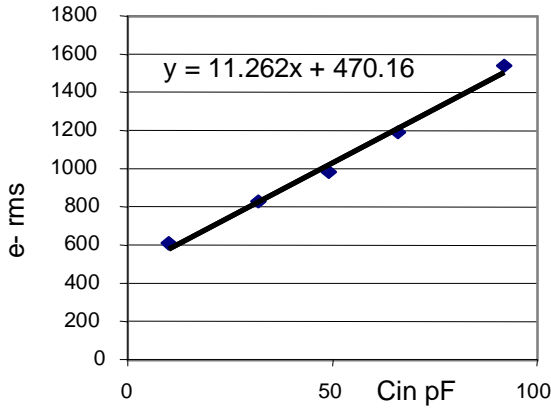


Fig 4: Noise versus input capacitance

### 3.2 Gain non-uniformity

The sensitivity (fig. 5) has been measured on 10 chips coming from 2 wafers; for these 160 channels, the gain has showed a rms spread of 0.05  $\text{mV/fC}$ , which is 1.36% of the mean value (3.675  $\text{mV/fC}$ ).

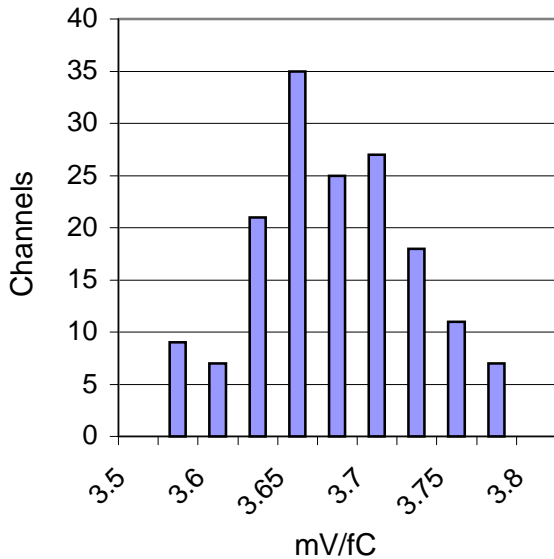


Fig 5: 160 channels gain spread

### 3.3 Dynamic range and linearity

The HMPID detector and the muon spectrometer need different characteristics of electronic circuitry amplification. The first one needs low noise and high sensitivity to be able to detect single photon emission; the second one requires low noise and large dynamic range to achieve precise measurements, for the localisation of the muon track.

For a maximum output voltage of 2 V, the aim has been to achieve at the same time the low noise and the largest dynamic range. The target characteristics correspond to the use of a 12-bit ADC.

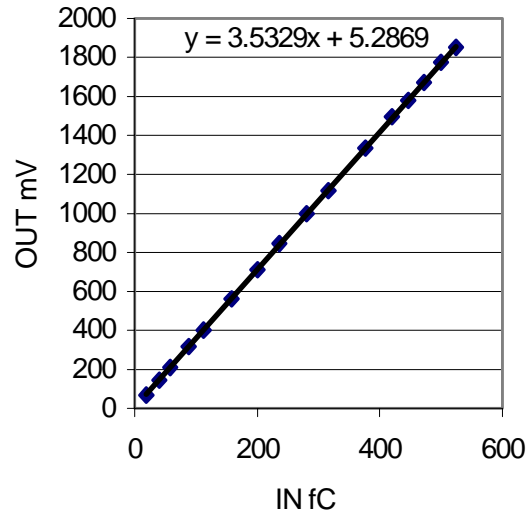


Fig. 6: Linearity

The full dynamic range shown in fig. 6 is 2 V for an input signal of 560  $\text{fC}$ . The non-linearity errors (fig. 7) are of the order of  $\pm 2$   $\text{fC}$  from 0 to 530  $\text{fC}$ . The negative range is limited to  $-1.1$  V, namely 300  $\text{fC}$ .

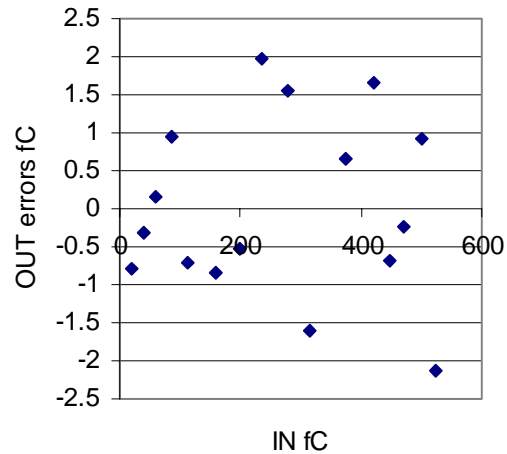


Fig. 7: Non-linearity errors

### 3.4 Pedestal distribution

Design parameter spread, essentially threshold voltage, causes pedestal variations of the 16 channels in a chip and between chip. On 10 chips (fig. 7), coming from 2 wafers, we have measured a difference of 6  $\text{mV}$  between the average values of pedestals; while the rms value of the pedestal spread on 160 channels is 13.5  $\text{mV}$ .

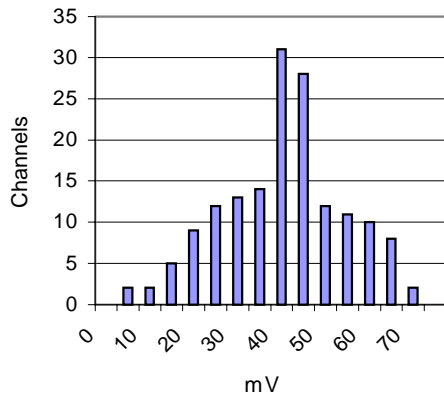


Fig 8: Pedestal distribution

### 3.5 Calibration

An analog multiplexer allows calibration of the chip channel per channel, through analog switches and individual 1 pF capacitors. However a parasitic injection, coming from the external circuitry, is added to the calibration signal. Figure 9 shows this parasitic effect with a 40 mV calibration input signal. Channel 1 and 2 are affected by this effect, while channel 14 reflects a layout defect.

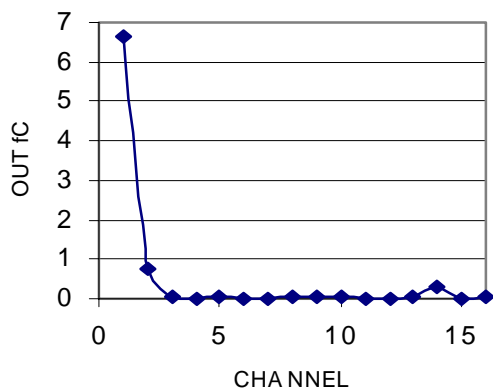


Fig 9: Parasitic injection

After having measured this effect, it is possible to know the relative accuracy of the gain. Figure 10 shows the results: the diamond points are the measured gain for a direct channel to channel injection through an external capacitance, the triangle points are the gain measured through the calibration input including the parasitic effect and the square points are the gain when the parasitic is deducted. One can see the good reproducibility of the internal 1 pF capacitors. The difference between direct signal injection and calibration signal injection is due to the discrepancy in the values of the external and internal capacitors.

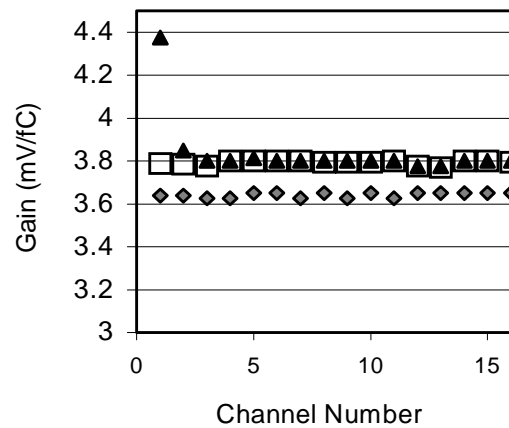


Fig. 10: Calibration

### 3.6 Peaking time adjustment

The peaking time can be adjusted from 1.1  $\mu$ s to 1.3  $\mu$ s by modifying the bias current of the shaper. With a value of 34  $\mu$ A, the peaking time is 1.2  $\mu$ s.

### 3.7 Silicon mode

An external DC level can switch off the deconvolution filter. In this case the Gassiplex07-2 can be connected directly to a Silicon detector if its leakage current is smaller than 1 nA, or through a capacitor if the current is bigger. The gain is reduced to 2.2 mV/fC and the dynamic range increased to 900 fC. Noise and linearity are not affected.

### 3.8 Radiation tolerance

An irradiation test has been made on one chip, using a Xray beam. The exposure was by step of 10 Krad up to 50 Krad; after each step measurements of pedestals, noise and power consumption have been made. All parameters increase by few %. A last step of 50 Krad caused a jump of 800 mV on the output DC level, but the chip was still working. After one week at 100  $^{\circ}$ C in a oven, all the parameters were recovered. Further tests on several samples are planned.

### 3.8 Pulse shaping on Gas Detector

The circuit has been tested on a Muon cathode pad gas detector using a  $^{55}$ Fe Xray source. One can see on fig. 11 that the return to the base line is almost perfect.

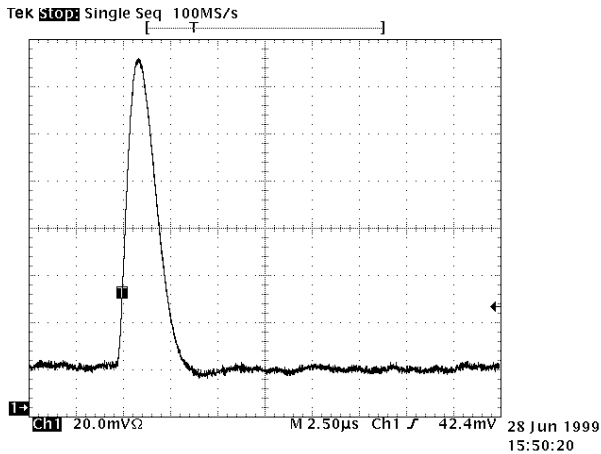


Fig. 11: Pulse shaping

### 3.9 Low power application

Depending on the application, the power consumption can be decreased by limiting the current bias in the CSA and in the buffers; at the cost of reduced noise performance and readout speed. At 4 mW/channel, the noise slope becomes  $15 e^- \text{ rms/pF}$  and the maximum readout speed will be 4 MHz.

### 3.10 Table of performances

Technology	Alcatel-Mietec-0.7 $\mu\text{m}$
Silicon area	$3.63 \times 4 = 14.5 \text{ mm}^2$
Gaseous detector mode	
Peaking time	1.2 $\mu\text{s}$
Peaking time adjust.	1.1 to 1.3 $\mu\text{s}$
Noise at 0 pF	530 $e^- \text{ rms}$
Noise slope	11.2 $e^- \text{ rms/pF}$
Dynamic range (+)	560 fC (0 to 2 V)
Dynamic range (-)	300 fC (0 to -1.1 V)
Gain	3.6 mV/fC
Non linearity	$\pm 2 \text{ fC}$
Baseline recovery	$\pm .5\%$ after 5 $\mu\text{s}$
Analog readout speed	10MHz (50 pF load)
Power consumption	8mW/chan. at 10 MHz
Output Temp Coeff.	0.05 mV/ $^{\circ}\text{C}$
Silicon detector mode	
Gain	2.2 mV/fC
Dynamic range (+)	900 fC (0 to 2 V)
Dynamic range (-)	500 fC (0 to -1.1 V)
Non linearity	$\pm 3 \text{ fC}$
Noise at 0 pF	600 $e^- \text{ rms}$
Noise slope	12 $e^- \text{ rms/pF}$
Low power mode	
Power consumption	4mW/chan. at 4 MHz
Noise at 0 pF	600 $e^- \text{ rms}$
Noise slope	15 $e^- \text{ rms/pF}$

## 4. CONCLUSIONS

The Gassiplex07-2 is a very flexible ASIC for a very wide range of detector readout applications. A 12-bit ADC has to be used to benefit from its low noise as well as its dynamic range. Analog multiplexing requires effective zero suppression and pedestal subtraction to retrieve information of channels hit by events. A companion ASIC, Dilogic-2, performs these operations; it can process 16, 32, 48 or 64 channels and can store up to 512 x 18-bit words in a on-chip asynchronous read-write FIFO. Samples will be available in October 99. Several packages can be used: ceramic LCC 48, QFP 44L plastic (10x10mm) and TQFP 48L (7x7mm). Concerning the ALICE detectors, the application being well defined, a new design iteration will be made in the coming months to make the logic levels compatible with the low level CMOS logic and also to reduce the number of biasing pins.

## 5. ACKNOWLEDGEMENTS

We would like to acknowledge Lambertus Van Koningsveld for his fruitful help in the use of different software.

## 6. REFERENCES

- [1] E. Beuville, K. Borer, E. Chesi, E. Heijne, P. Jarron, B. Lisowski and S. Singh, AMPLEX, A low noise, low power analog CMOS signal processor for multi-element particle detectors, Nucl. Instrum. Methods Phys. Res. **A288** (1990) 157.
- [2] J.C. Santiard, W. Beusch, S. Buytaert, C.C. Enz, E. Heijne, P. Jarron, F. Krummenacher, K. Marent and F. Piuz, GASPLETEX, A low noise analog signal processor for readout of gaseous detectors, CERN-ECP/94-17.
- [3] CERN/LHCC 98-19, ALICE TDR1, Detector For High Momentum Particle Identification, edited by E. Nappi, G. Paic, F. Piuz, August 1998 ISBN 92-9083-134-0
- [4] "The forward muon spectrometer. Addendum to the ALICE Technical Proposal" CERN/LHCC 96-32, LHCC/P3-Addendum 1
- [5] R.A. Boie, A.T. Hrisoho and P. Rehak, Signal shaping and tail cancellations for gas proportional detectors at high counting rates, Nucl. Instrum. Methods Phys. Res. **192**(1982) 365-374.